coatings

MDPI

Article

A Self-Healing Coating with UV-Shielding Property

Lei Peng [1,*], Musong Lin [1], Sheng Zhang [2], Li Li [1], Qiang Fu [1] and Junbo Hou [2]

[1] Electric Power Research Institute of Guangdong Power Grid, Guangzhou 510080, China
[2] State Key Laboratory of Polymer Materials Engineering, Sichuan University, Chengdu 610065, China
* Correspondence: penglei1025@whu.edu.cn

Received: 22 May 2019; Accepted: 27 June 2019; Published: 1 July 2019

Abstract: A self-healing coating with UV-shielding property was prepared in this paper. The self-healing property was based on the inclusion between a host (β-CD-TiO_2) and a guest HEMA-Ad). After inclusion of the host and guest, the host–guest complex (HEMA-Ad/β-CD-TiO_2) was polymerized with other reactive monomers (HEMA and BA) to obtain the final coating. The coating had good hydrophobicity (water contact angle >90°, moisture absorption rate <2%) and excellent UV-shielding performance (ultra-violet protect factor >90%), and could be firmly bonded to a soft substrate. In addition, the coating had good self-healing property, which means that cracks in the material can recover many times after being damaged and that the UV-shielding ability can be fully restored with the self-healing process.

Keywords: coating; self-healing; UV-shielding; host–guest

1. Introduction

When an ordinary substrate is used outdoors, ultraviolet radiation will cause a series of photodegradation reactions, resulting in fading and a decrease in the mechanical properties of the substrate, thereby greatly shortening its life-span. If a layer of UV-shielding coating is applied on the surface of such a substrate, it can be well protected from UV radiation. On the other hand, tiny mechanical scratches can damage the coating and reduce its protective effects. For example, in the field of power cables, the outer surface of the cable often accumulates tiny cracks due to dragging (or other installation actions) and photoaging (usually ultraviolet light), which allows penetration of moisture and oxygen, affecting the life-span of the cable. A UV-shielding coating with self-healing effect can prevent the substrate from being damaged (i.e., the damage can be eliminated by self-healing of the coating) and can delay its aging by ultraviolet irradiation, thereby improving the service life-span of the substrate.

A self-healing material is a kind of smart material that can heal itself when damaged [1]. According to their different healing principles, they are mainly divided into two categories. One is the filling type, which exhibits the self-healing property via carriers that are dispersed in its polymer matrix, such as microcapsules [2–4], hollow fibers [5,6] and microvasculatures [7,8]. However, it is difficult for such materials to achieve repeated healing due to the limited capacity of the carriers. The other kind is the intrinsic type, which heal wounds through the intermolecular interactions (including covalent and non-covalent bonds) of their components. For materials that rely on covalent bonds to self-heal, the covalent bonds can be reversibly broken and generated under heat [9], light [10] and pH [11] treatments, allowing for the healing of damaged parts. For materials that rely on non-covalent bonds to self-heal, they do not require external stimulus factors to activate the self-repair property, and mainly depend on non-covalent bonds such as hydrogen bonding [12], π–π interaction [13], metal coordination [14] and topology structure [15] to form stable supramolecular structures. The advantage of these materials is that they can self-heal multiple times and are not restricted by the capacity of

carriers. Among these supramolecular materials, the host–guest model has excellent self-healing effects. A research group led by Professor Huang developed a line of supramolecular gels based on the host–guest interaction. Their gels were capable of self-healing quickly with 10,000% deformation [16]. Mynar et al. prepared a self-healing gel by the inclusion interaction of clay and telechelic dendritic macromolecules with multiple bonded ends, which was able to 100% self-heal [17]. Zhang et al. fabricated a self-healing elastomer with excellent mechanical properties and demonstrated its ability to restore 90% of its mechanical strength [18].

In order to prepare a coating that had both self-healing and UV-shielding properties, we selected a polymer material comprised of a host–guest inclusion compound. Cyclodextrin grafted with titanium dioxide nanoparticles (ultraviolet shielding agent) was used as the host molecule, and adamantane grafted with a reactive monomer was used as the guest molecule. After the inclusion of the host molecules and guest molecules, the host–guest complex was polymerized with other reactive monomers to obtain a self-healing coating with UV-shielding property.

2. Principle

When the coating β-CD-TiO_2/P(HEMA-co-BA) is mechanically damaged, there is dissociation of the inclusion interaction between host–guest molecules, resulting in many free host and guest molecules in the wound cross-section. After contact with moisture, the cross-section expands, causing the two sides to touch each other. In this situation, the polymer molecular chains can become entangled with one another, and the free host and guest molecules on the cross-section are re-integrated. With the coaction of chain entanglement and host–guest interaction, the coating finally completes self-healing (as shown in Figure 1).

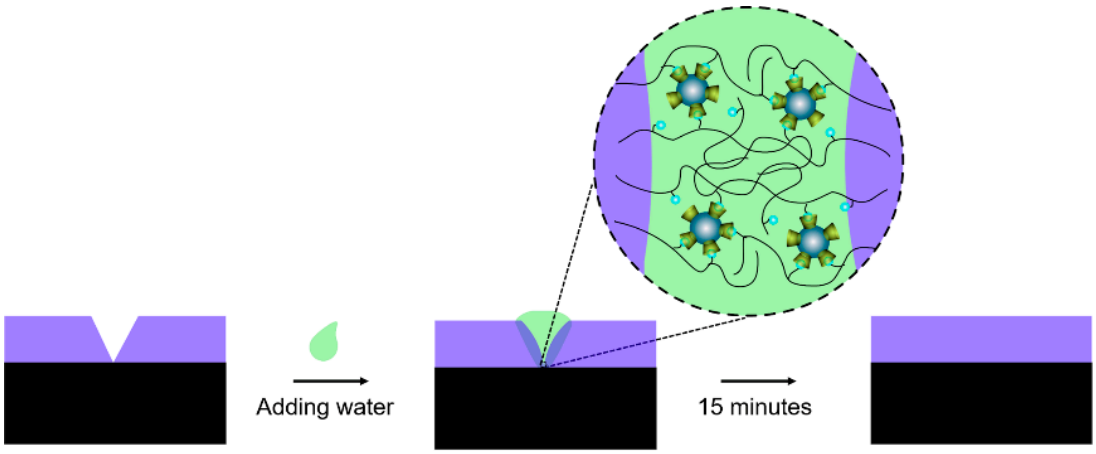

Figure 1. Self-healing mechanism of β-CD-TiO_2/P(HEMA-co-BA).

3. Materials and Methods

3.1. Materials

2-Hydroxyethyl-methacrylate (HEMA), β-cyclodextrin (β-CD), butyl acrylate (BA), azobisisobutyronitrile (AIBN, 99%, recrystallization), TiO_2 nanoparticles (10.5 nm), and adamantanecarboxylic acid (Ad–COOH) were obtained from Aladdin Reagent Co., Ltd (Shanghai, China). All the above-mentioned materials were analytically pure.

3.2. Sample Fabrication

3.2.1. Preparation of the Guest Molecule 2-Hydroxyethyl-methacrylate-adamantane (HEMA-Ad)

We dissolved 2.3 g of Ad–COOH in 20.0 mL of thionyl chloride, followed by stirring at 80 °C for 2 h, after which the unreacted thionyl chloride was removed by rotary evaporation to obtain adamantyl chloride. Then, the adamantyl chloride was dissolved in 100 mL of anhydrous dichloromethane and added dropwise to a mixed solution containing 1.0 mL of HEMA and 1.6 mL of triethylamine at 0 °C. After reacting for 5 h, the pale yellow solution obtained was washed successively with 100 mL of 1 M HCl solution, 1 M $NaHCO_3$ solution and water. After dehydration (by anhydrous sodium sulfate) and drying, HEMA-Ad was obtained. The crude product obtained was purified by flash column chromatography (the eluent was a mixed solution of n-hexane and ethyl acetate in a volume ratio of 40:1) to obtain a pale yellow oily liquid, which was allowed to stand for a period of time to obtain a solid particle precipitate.

3.2.2. Preparation of the Host Molecule β-CD-TiO_2

β-CD-TiO_2 was prepared by a UV-irradiation method (improved according to the method reported in Reference [19]). The procedure was as follows: TiO_2 nano-particles were dispersed in a β-CD aqueous solution through ultrasonic vibration for 45 min. The resulting solution was then irradiated under ultraviolet light for 48 h at room temperature and centrifuged to obtain a solid product. After washing three times with ultrapure water, it was freeze-dried to obtain β-CD-TiO_2.

3.2.3. Preparation of the β-CD-TiO_2/P(HEMA-co-BA) Coating

We added 213 mg β-CD-TiO_2 and 10 mg HEMA-Ad to 6.0 mL water for 30 min of ultrasonic vibration. The mixture was then stirred at room temperature for 24 h, and freeze-dried to obtain a HEMA-Ad/β-CD-TiO_2 inclusion compound. Then, the HEMA-Ad/β-CD-TiO_2 was dispersed into 6.0 mL of ethanol with ultrasonic vibration for 45 min. After that, 1.0 mL of HEMA, 1.2 mL of BA and 5.0 mg of AIBN were added. Under stirring, the mixture was polymerized at 55 °C in a protective atmosphere of argon for 12 h to produce a white viscous polymer solution; that is, the anti-ultraviolet self-healing coating β-CD-TiO_2/P(HEMA-co-BA). The preparation process is shown in Figure 2.

3.3. Sample Characterization and Application

^1H and ^{13}C NMR spectra (Avance Bruker-600, Rheinstetten, Germany), mass spectra (Finnigan LCQDECA, Thermo Fisher Scientific, Waltham, MA, USA), FT-IR (Nicolet 560, Austin, TX, USA), XPS (ESCALAB 250Xi, Thermo Fisher Scientific, Waltham, MA, USA), XRD (EMPYREAN, Almelo, Netherlands), and SEM (SIGMA 300, Zeiss, Oberkochen, Germany) were used to characterize the inclusion complex formed by the host and guest. The water contact angle was used to measure the hydrophobicity of the coating. UV-Vis spectra (Varioskan Flash, Thermo Fisher Scientific, Waltham, MA, USA) and FT-IR spectra were used to measure the UV shielding performance. A super-resolution confocal microscope (KEYENCE, Osaka Prefecture Japan) and SEM were used to detect the self-healing effect.

When the coating was prepared, it was coated on the surface of substrates. After about 50 min, most of the solvent (ethanol) volatilized to form a uniform protective film on the surface of the substrates. Then, the coated substrates were dried at 30 °C for 6 h and at 60 °C for 8 h to obtain substrates with self-healing coatings.

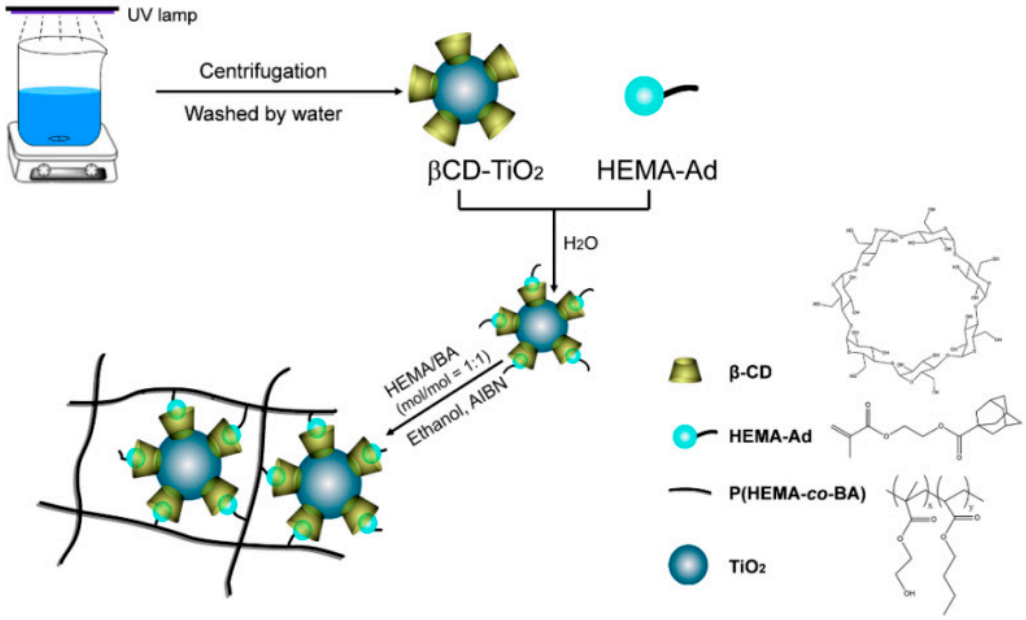

Figure 2. Schematic of the preparation process of β-CD-TiO_2/P(HEMA-co-BA).

4. Results and Discussion

4.1. Characterization of β-CD-TiO_2/P(HEMA-co-BA)

4.1.1. Characterization of β-CD-TiO_2 and HEMA-Ad

In this work, β-CD-TiO_2 was prepared via a UV-irradiation method (described in Section 3.2.2). FT-IR and XPS spectra were used to verify if the β-CD molecules successfully modified the surface of the TiO_2 nanoparticles. From the FT-IR spectra (shown in Figure 3a), both TiO_2 and β-CD-TiO_2 had strong absorption peaks at 668 cm^{-1} due to the presence of Ti–O–Ti bonds. Furthermore, the absorption peaks of β-CD-TiO_2 at 2922, 1166 and 1064 cm^{-1} were found to correspond to the stretching vibration of a C–H bond, stretching vibration of a C–O bond and anti-symmetric vibration of a C–O–C bond, respectively. Compared with the XPS spectrum of TiO_2, that of β-CD-TiO2 exhibited new bonds of C–OH and C=O in the O1*s* region. The C–OH bond was derived from glucose units in β-CD, while the C=O bond was likely derived from the oxidation of hydroxyl groups in β-CD (the holes generated on the surface of TiO_2 nanoparticles oxidized the hydroxyl groups in β-CD during UV irradiation). The combined characterization by FT-IR and XPS analyses indicated that β-CD could be successfully attached to the surface of TiO_2 nanoparticles by UV irradiation. Moreover, XRD results indicated that the β-CD molecule on the surface of TiO_2 did not affect the crystal form of the TiO_2 nanoparticles (as shown in Figure 3d), thereby ensuring the functionality of the TiO_2 nanoparticles (i.e., UV-shielding).

Thermogravimetric analysis (TGA) was used to estimate the content of β-CD in β-CD-TiO_2. Then, the number of β-CD molecules that attached on the surface of each TiO_2 nanoparticle was calculated (as shown in Figure 4). Based on the TGA results of TiO_2 and β-CD-TiO_2, we calculated that β-CD content in β-CD-TiO_2 was 0.012 mmol/g, and there were about 138 β-CD molecules on the surface of each TiO_2 nanoparticle (according to Reference [20]).

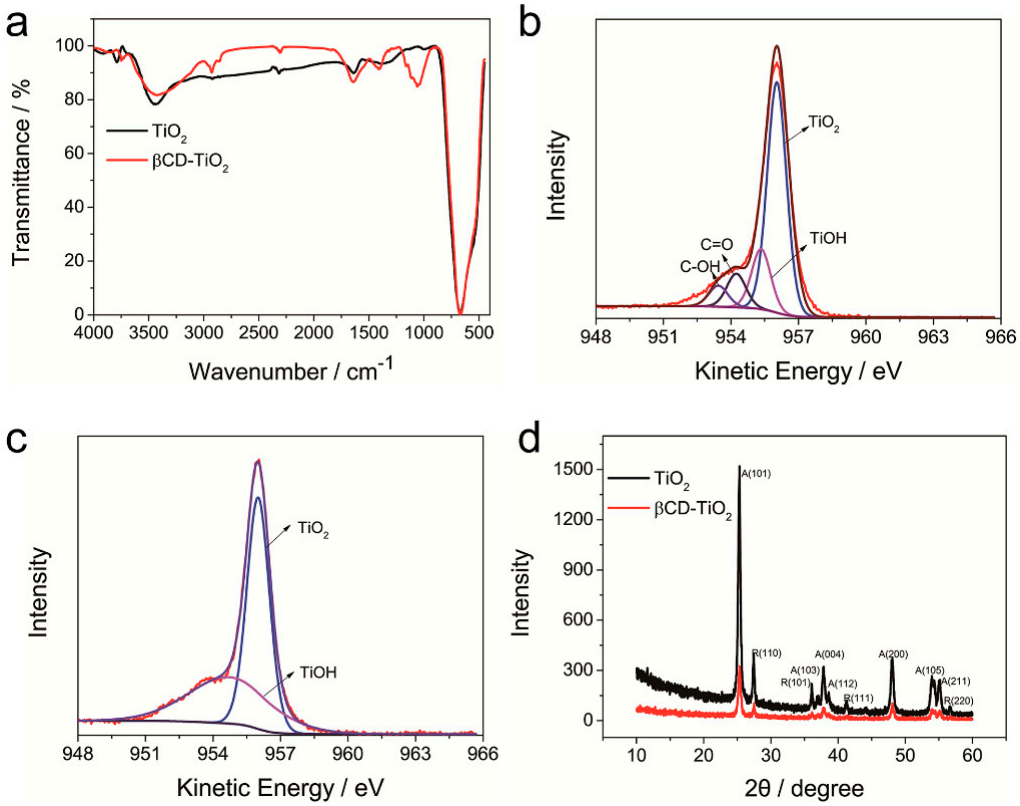

Figure 3. Spectra of β-CD-TiO_2 and TiO_2: (**a**) FT-IR spectrum of TiO_2 and β-CD-TiO_2; (**b**) XPS spectrum of β-CD-TiO_2 in the O1s interval; (**c**) XPS spectrum of TiO_2 in the O1*s* interval; (**d**) XRD spectrum of TiO_2 and β-CD-TiO_2.

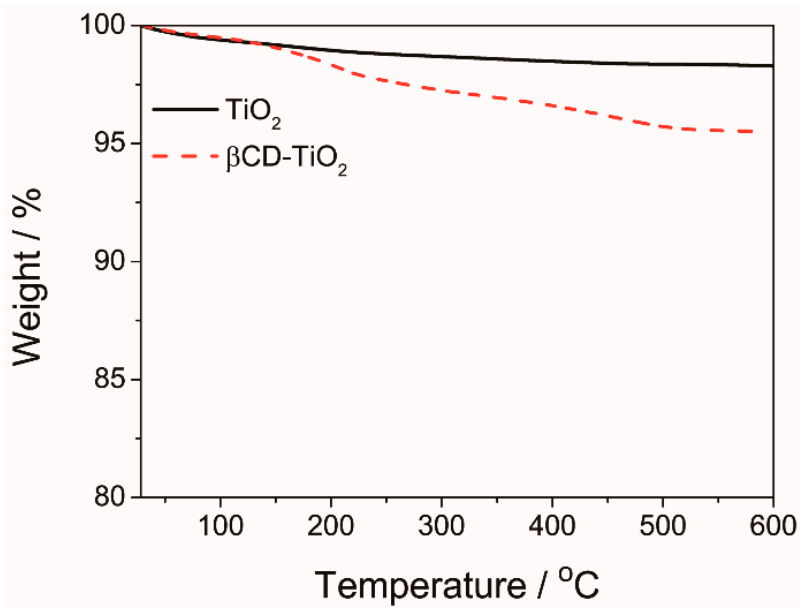

Figure 4. Thermogravimetric analysis (TGA) of TiO_2 and β-CD-TiO_2.

In order to test the effect of adamantane grafted with HEMA, the ^{1}H NMR and ^{13}C NMR spectra of the guest molecule HEMA-Ad were analyzed (shown in Figure 5).

In Figure 5a, there are signal peaks at δ 6.09 (s, 1H), 5.55 (s, 1H), 4.31 (t, 2H), 4.26 (t, 2H), and 1.68–1.92 (m, 15H). The peaks at 6.09 and 5.55 ppm correspond to the hydrogen atoms in the olefinic bond of 2-hydroxyethyl-methacrylate, and the ratio of their peak area is 1:1. The peaks at 4.31 and

4.26 ppm (position "4" and "5") correspond to the methylene hydrogens that are adjacent to the ester bond, and the ratio of their peak area is also 1:1, indicating the formation of ester bonds. The peak at 1.77 ppm corresponds to the hydrogen atom at the methylene (position "9") in adamantane, and the ratio of the peak area of position "9" and "1" is 6:1, which is in accordance with the hydrogen number ratio of HEMA-Ad. This indicated that the HEMA-Ad product was successfully prepared.

As shown in Figure 5b, the two peaks at 177.40 and 167.30 ppm correspond to the two carbonyl carbons, while the 136.01 and 125.90 ppm peaks correspond to the two carbons in the double bond. The peaks at 62.40 and 61.71 ppm correspond to the two carbon atoms on $–OCH_2CH_2O–$. The four peaks from 38.59 to 27.88 ppm correspond to the four types of carbon atoms in adamantane. The peak at 18.17 mmp corresponds to the methyl at position "2". These findings also demonstrated the successful preparation of HEMA-Ad.

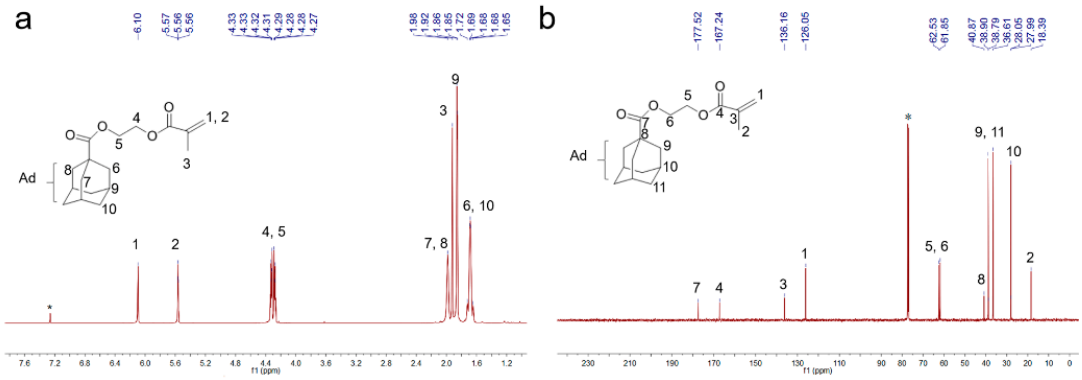

Figure 5. 2-Hydroxyethyl-methacrylate-adamantane (HEMA-Ad) spectra: (**a**) ^{1}H NMR spectrum; (**b**) ^{13}C NMR spectrum.

4.1.2. Polymerization of β-CD-TiO_2/P(HEMA-co-BA)

The polymerization of HEMA-Ad, β-CD-TiO_2, HEMA, and BA were carried out in ethanol. Comparing the FT-IR spectra before and after polymerization (shown in Figure 6), we found that the absorption peaks of C=C after polymerization ($\nu_{C=C}$ 1636 cm^{-1}, $\nu_{=CH}$ 985/948 cm^{-1} and $\nu_{=CH}$ 903/886 cm^{-1}) disappeared, indicating that the polymerization reaction proceeded smoothly.

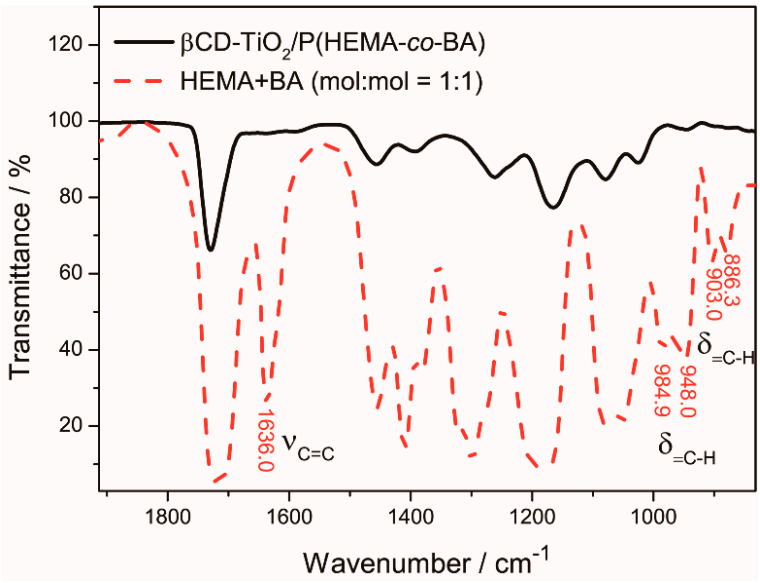

Figure 6. FT-IR spectra of monomer (HEMA + BA) and polymer β-CD-TiO_2/P(HEMA-co-BA).

4.2. Mechanical Properties and Wear Resistance of Coatings

In order to test the mechanical properties of this coating, a stress–strain curve was used for evaluation. It can be seen from Figure 7a that the maximum tensile strength of the P(HEMA-co-BA) was 2.03 MPa, and it increased to 2.69 MPa when TiO_2 nanoparticles were added. Compared with the two, the maximum tensile strength increased to 4.50 MPa with the addition of HEMA-Ad/β-CD-TiO_2 inclusion complex, meaning that the addition of HEMA-Ad/β-CD-TiO_2 significantly enhanced the mechanical properties of the coating. This is mainly due to the addition of the host–guest inclusion complex: The surface of HEMA-Ad/β-CD-TiO_2 has a plurality of bonds which can participate in the polymerization reaction, and act as "crosslinking agents" in the polymerization process to enhance the network structure of the coating.

Wear resistance is an important indicator for evaluating the mechanical stability of coatings. We used a sandpaper friction test method to evaluate the wear resistance of the coatings according to the test method for rubber wear resistance. After the coating was formed on the base material, the sandpaper (with a weight of 1 kg) was dragged 20 cm in 15 s to calculate the mass loss rate (MLR). The lower the MLR, the better the wear resistance. As shown in Figure 7b, the MLR value of the P(HEMA-co-BA), TiO_2/P(HEMA-co-BA) and β-CD-TiO_2/P(HEMA-co-BA) coatings were measured. The results showed that the MLR value of P(HEMA-co-BA) and TiO_2/P(HEMA-co-BA) were higher than that of the self-healing coating, which meant the scratch resistance of the coating without utilization of the self-healing effect was not as good as that of the self-healing coating. This can be explained by two factors. Firstly, the organic molecules (β-CD + HEMA-Ad) were modified on the surface of TiO_2 nanoparticles to improve their compatibility with the polymer networks of the self-healing coating. Secondly, the host and guest groups acted as a cross-linking agent during the polymerization process, which not only improved the stability of the nanoparticles in the polymer network, but also significantly enhanced the overall mechanical properties of the coating. Therefore, the β-CD-TiO_2/P(HEMA-co-BA) coating exhibits the best wear resistance.

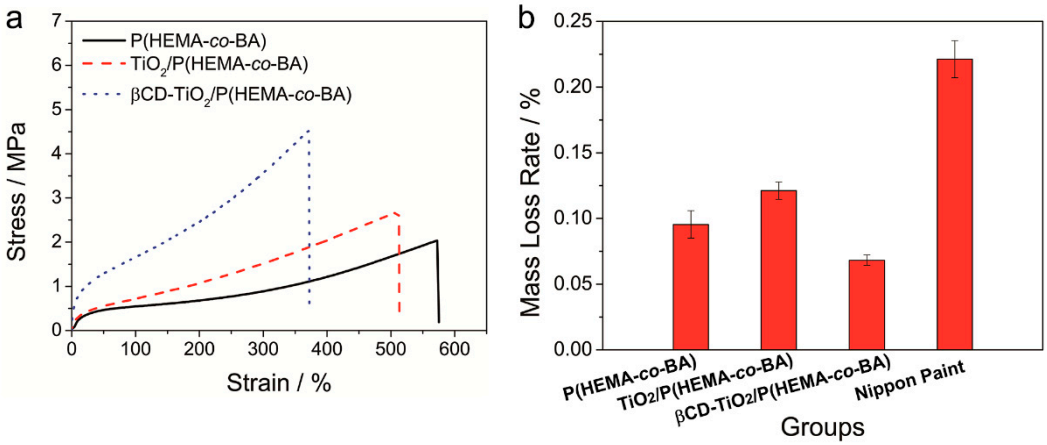

Figure 7. Mechanical properties and wear resistance of coatings: (**a**) Stress–strain curves of P(HEMA-co-BA), TiO_2/P(HEMA-co-BA) and β-CD-TiO_2/P(HEMA-co-BA); (**b**) comparison of mass loss rate between self-made coatings and commercial coating (Nippon paint).

4.3. Adhesion of Coating

In order to detect the adhesion of the coating on the substrate, the substrates that were coated with the β-CD-TiO_2/P(HEMA-co-BA) coating were twisted and bent to observe if any coating peeled off. As shown in Figure 8, the coating did not fall off after one or more bending actions, and there were no micro-cracks on the curved surface, indicating that the β-CD-TiO_2/P(HEMA-co-BA) coating adhered well on the surface of the substrates.

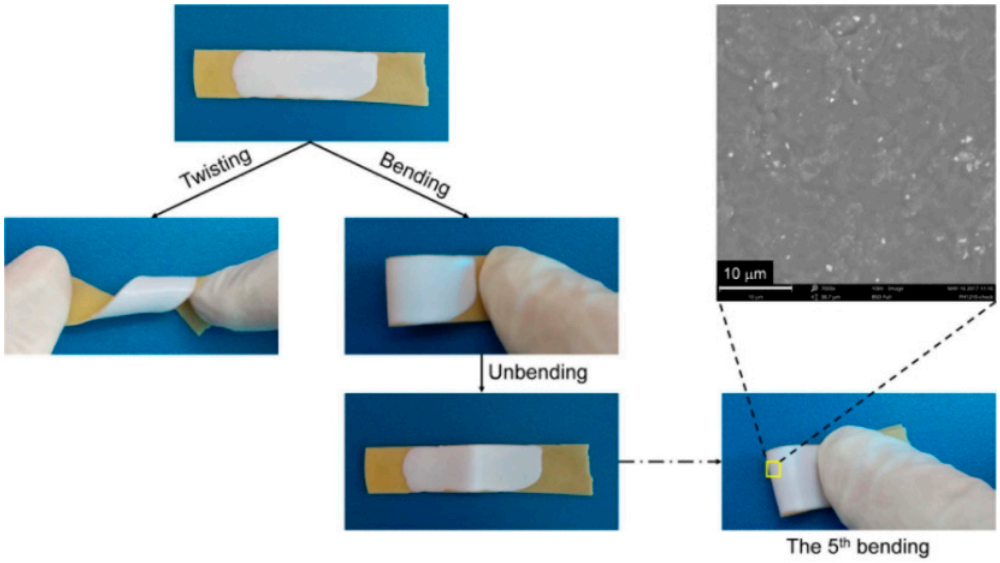

Figure 8. Twisting and bending of a coated substrate.

4.4. Hydrophobicity and Hygroscopicity of Coatings

The hydrophobic properties of the coating were measured by water contact angle and moisture absorption. The water contact angle and moisture absorption rate of the coating under different humidity conditions were measured, as shown in Figures 9 and 10. It can be seen from Figure 9 that even if the β-CD-TiO_2/P(HEMA-co-BA) coating was placed in an environment with a humidity of 76% RH, it maintained a hydrophobic surface (water contact angle >90°). This is because after polymerization of HEMA (CH_2=$CCH_3COOCH_2CH_2OH$) and BA ($CH_2CHCOOC_4H_9$), a large amount of –CH_2– exists in the molecular chain, which has a hydrophobic role. On the other hand, the moisture sorption ratio of the coating was only 2.0% when it was in an environment with a humidity of 54% RH (as seen in Figure 10), indicating that the coating almost does not absorb moisture from the air under normal circumstances. However, in a high humidity environment (such as 100% RH), the moisture sorption ratio of this coating increased to a certain extent.

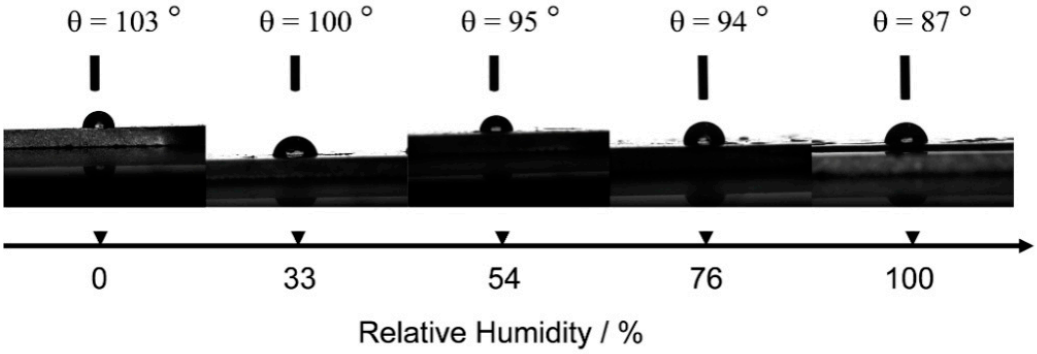

Figure 9. Water contact angle of the β-CD-TiO_2/P(HEMA-co-BA) coating under different humidity conditions.

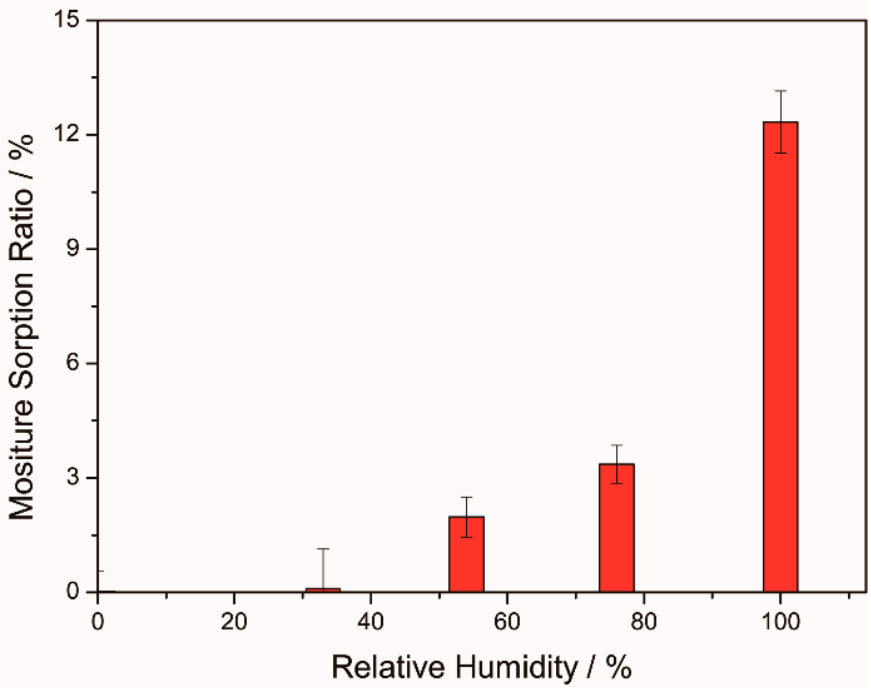

Figure 10. Moisture sorption ratio of the β-CD-TiO_2/P(HEMA-co-BA) coating under different humidity conditions.

4.5. Coating UV-Shielding Performance

The UV-shielding performance of the β-CD-TiO_2/P(HEMA-co-BA) coating was measured by UV-Vis spectroscopy. As shown in Figure 11a, the β-CD-TiO_2/P(HEMA-co-BA) coating exhibited a strong absorption capacity (absorption rate >90%) in the range of 200–350 nm. This excellent UV absorption capacity is derived from the added TiO_2 nanoparticles: On one hand, TiO_2 can absorb ultraviolet light with energy higher than its band gap (3.0 eV for band gap of rutile TiO_2 and 3.2 eV for anatase TiO_2); on the other hand, due to the high refractive index of the surface of the TiO_2 nanoparticles, ultraviolet rays that are outside the absorption range can be "consumed" by scattering.

UV accelerated aging experiments were used to verify the UV-shielding effect of the β-CD-TiO_2/P(HEMA-co-BA) coating. As shown in Figure 11b, the initial PVC sample was colorless and transparent (Sample I). However, the color of the PVC sample without the coating changed to brown under the ultraviolet accelerated aging test (Sample III). Moreover, the FT-IR spectrum of Sample III, shown in Figure 11c, exhibited a strong absorption near 1659 cm^{-1}, indicating a large amount of carbonyl formed in the PVC. The UV-Vis spectrum of Sample III (Figure 11d) showed a strong absorption in the range of 220–300 nm, indicating that conjugated structures were formed in the PVC. These results indicate that Sample III experienced a relatively severe degradation reaction. In contrast to Sample III, the PVC sample coated by β-CD-TiO_2/P(HEMA-co-BA) (Sample II) remained colorless under the ultraviolet accelerated aging test. Moreover, not only was the appearance essentially consistent with Sample I, but so too was the FT-IR and UV-Vis spectra, despite Sample I not undergoing ultraviolet accelerated aging. This indicates that the β-CD-TiO_2/P(HEMA-co-BA) coating on Sample II had a good UV-shielding performance.

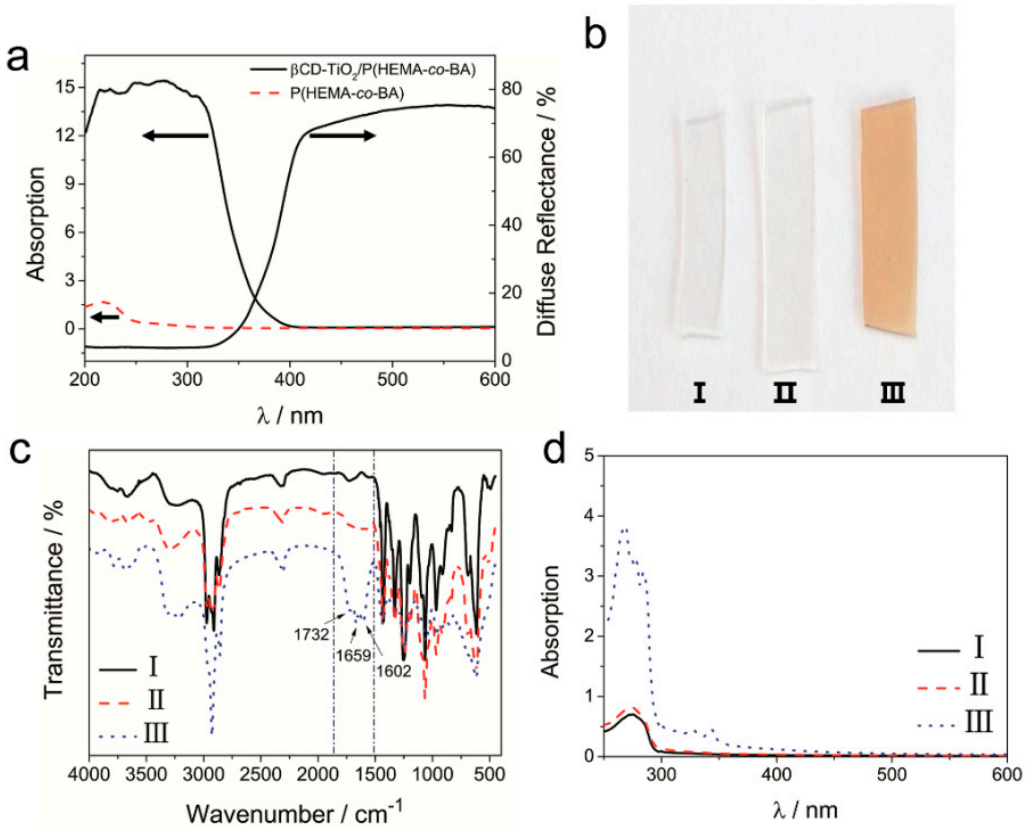

Figure 11. UV-shielding properties of the β-CD-TiO_2/P(HEMA-co-BA) coating: (**a**) UV-Vis absorption and diffuse reflectance spectroscopy; (**b**) photographs of three sample strips; (**c**) FT-IR spectra of three samples; (**d**) UV-Vis absorption spectra of three samples (I: PVC initial sample; II: PVC sample subjected to UV-vis accelerated aging with coating; III: PVC sample subjected to UV-vis accelerated aging without coating).

4.6. Self-Healing Properties

4.6.1. Self-Healing of Mechanical Property

To evaluate the self-healing properties of the coating, a super-resolution confocal microscope was used to observe its surface. As shown in Figure 12a, the cross-sectional area of the wound on the surface of the coating was about 7282 μm^2 before self-healing. When 20 μL of water was added to the wound surface and 15 min was allowed to pass, the cross-sectional area of the wound changed to 0 μm^2 (i.e., the wound almost disappeared). In order to observe the self-healing properties of the coating more intuitively, SEM was used to observe the wound. As shown in Figure 12b, the wound was able to heal itself after a period of time, indicating that the β-CD-TiO_2/P(HEMA-co-BA) coating did have the ability of self-healing.

In Figure 13, the self-healing ability of the β-CD-TiO_2/P(HEMA-co-BA) coating is shown to occur multiple times, as the coating is subjected to at least three self-healing events at the same position. This is because the self-healing ability of the coating is derived from the entanglement of the molecular chains and the host–guest inclusion, both of which are reversible. Thus, the coating can perform multiple self-healing episodes.

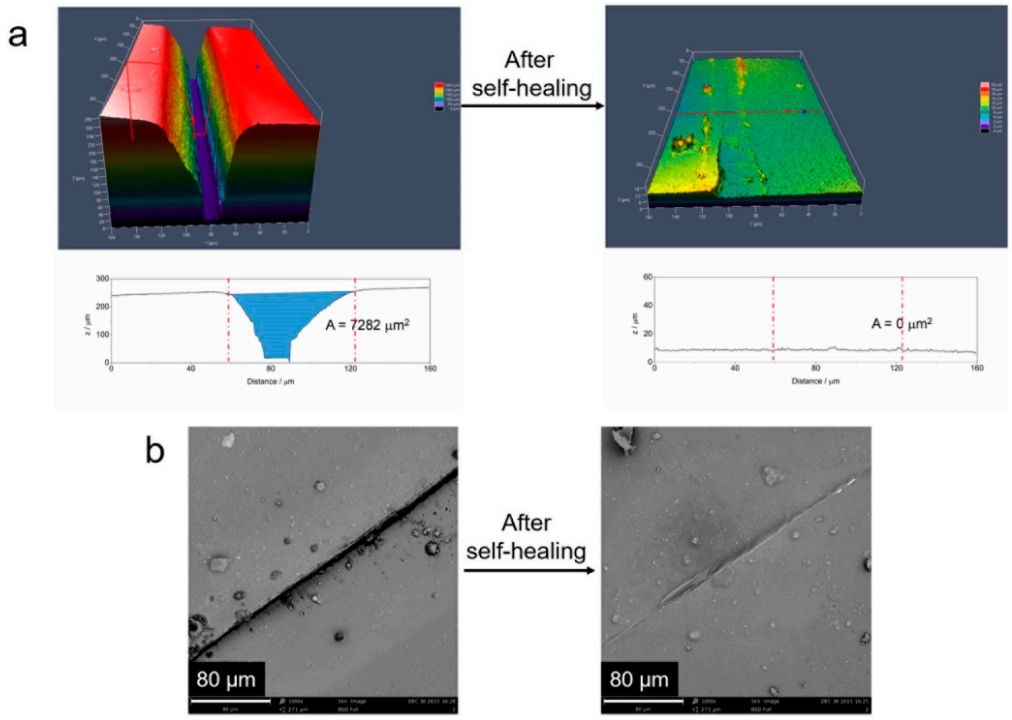

Figure 12. Self-healing properties of the β-CD-TiO_2/P(HEMA-co-BA) coating: (**a**) Super-resolution confocal microscope images of the coating before and after self-healing—the upper image is a contour view and the lower image is a cross-sectional view; (**b**) SEM image of the coating before and after self-healing.

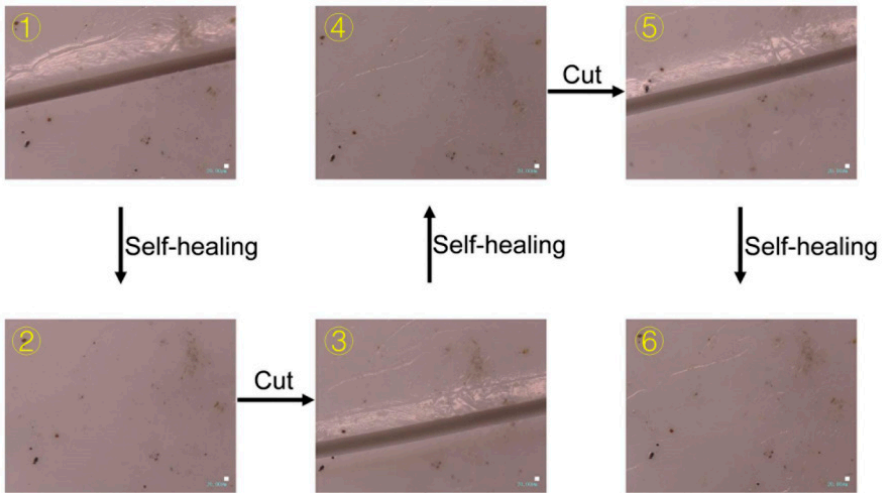

Figure 13. Multiple self-healing of the β-CD-TiO_2/P(HEMA-co-BA) coating.

4.6.2. Self-Healing of UV-Shielding Property

The UV degradation of rhodamine B (Rh B) was used to evaluate the coatings' self-healing of the UV-shielding property, as Rh B degrades under UV irradiation and its concentration can be measured by fluorometry. Firstly, the outer surfaces of two identical quartz tubes were coated with the β-CD-TiO_2/P(HEMA-co-BA) coating, after which an equal number of scratches were made on the surface of the coating. Then, the tubes were divided into two groups: The first group (UV-1) was covered with wet filter paper on the coating for 24 h to self-heal; the second group (UV-2) was placed in a dry place (in this case, it is difficult for the coating to self-heal) so that the surface remained

scratched after 24 h. Next, an equal amount of the Rh B solution was added to UV-1 and UV-2, and the concentration of Rh B was detected after ultraviolet irradiation for a certain period of time. The results are shown in Figure 14. It can be seen that the degradation rate of Rh B in UV-2 was 25%, indicating that if the wound is not healed, the UV-shielding ability of the coating will be reduced. In contrast, the concentration of Rh B in UV-1 was the same as the original concentration, indicating that the coating completely shielded the ultraviolet radiation; that is, the UV-shielding ability of the coating is completely restored after self-healing.

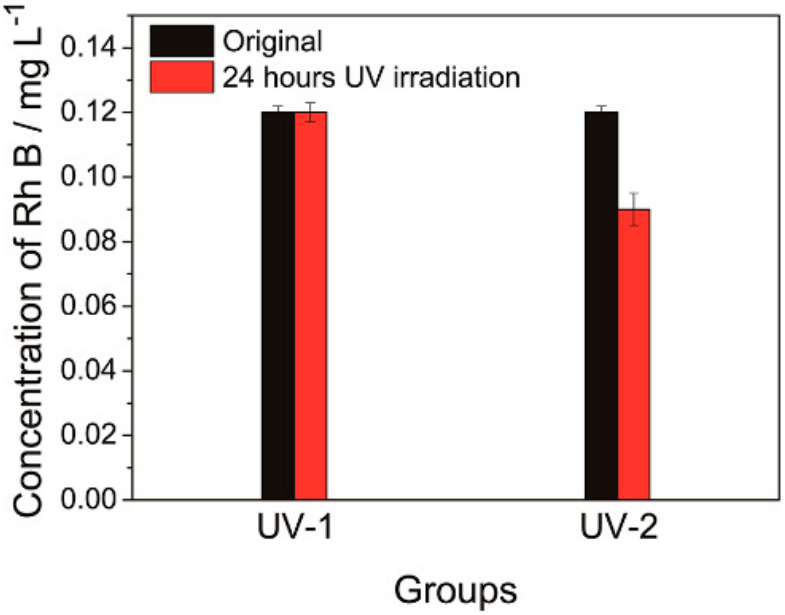

Figure 14. UV degradation test of rhodamine B (Rh B): Changes in Rh B concentration of UV-1 and UV-2 after UV irradiation.

5. Conclusions

A novel UV-shielding coating with self-healing properties was prepared. The coating was synthesized by radical polymerization using HEMA, BA and a host–guest assembly (β-CD-TiO_2 nanoparticles acted as the host, while HEMA-Ad acted as the guest). The introduction of the host–guest inclusion complex in the coating not only enhanced the compatibility of the nanoparticles in the polymer network, but also acted as a "cross-linking agent" in the polymerization process, which significantly enhanced the mechanical properties and wear resistance of the coating. The coating had good hydrophobic property (water contact angle >90° at normal humidity) and UV-shielding property (UV absorption rate >90% in the range of 200–350 nm), and adhered well on the surface of substrate. With the coaction of chain entanglement and host–guest interaction, the coating was able to heal the wound spontaneously multiple times in the same location. In addition, the UV-shielding ability was fully restored with the self-healing process.

Author Contributions: Conceptualization, L.P., M.L. and S.Z.; Methodology, Lei Peng; Formal Analysis, L.L., Q.F. and J.H.; Writing-Original Draft Preparation, L.P.

Funding: This research is supported by China Postdoctoral Science Foundation Grant (2018M630920) and China Southern Power Grid project (No. GDKJQQ20152049).

Conflicts of Interest: The authors declare no conflict of interest.

References

1. Mynar, J.L.; Aida, T. Materials science: The gift of healing. *Nature* **2008**, *451*, 895. [CrossRef] [PubMed]
2. White, S.R.; Sottos, N.R.; Geubelle, P.H.; Moore, J.S.; Kessler, M.; Sriram, S.R.; Brown, E.N.; Viswanathan, S. Autonomic healing of polymer composites. *Nature* **2001**, *409*, 794. [CrossRef] [PubMed]
3. Keller, M.W.; White, S.R.; Sottos, N.R. A self-healing poly (dimethyl siloxane) elastomer. *Adv. Funct. Mater.* **2010**, *17*, 2399–2404. [CrossRef]
4. Rule, J.D.; Brown, E.N.; Sottos, N.R.; White, S.R.; Moore, J.S. Wax-protected catalyst microspheres for efficient self-healing materials. *Adv. Mater.* **2005**, *17*, 205–208. [CrossRef]
5. Bleay, S.M.; Loader, C.B.; Hawyes, V.J.; Humberstone, L.; Curtis, P.T. A smart repair system for polymer matrix composites. *Compos. Part A Appl. Sci. Manuf.* **2001**, *32*, 1767–1776. [CrossRef]
6. Tras, R.S.; Williams, G.J.; Bond, I.P. Bioinspired selfhealing of advanced composite structures. *JR Soc. Interface* **2007**, *4*, 363–371. [CrossRef] [PubMed]
7. Toohey, K.S.; Sottos, N.R.; Lewis, J.A.; Moore, J.S.; White, S.R. Self-healing materials with microvascular networks. *Nat. Mater.* **2007**, *6*, 581. [CrossRef] [PubMed]
8. Toohey, K.S.; Hansen, C.J.; Lewis, J.A.; White, S.R.; Sottos, N.R. Delivery of two-part self-healing chemistry via microvascular networks. *Adv. Funct. Mater.* **2009**, *19*, 1399–1405. [CrossRef]
9. Chen, X.; Wudl, F.; Mal, A.K.; Shen, H.; Nutt, S.R. New thermally remendable highly cross-linked polymeric materials. *Macromolecules* **2003**, *36*, 1802–1807. [CrossRef]
10. Ling, J.; Rong, M.Z.; Zhang, M.Q. Coumarin imparts repeated photochemical remendability to polyurethane. *J. Mater. Chem.* **2011**, *21*, 18373–18380. [CrossRef]
11. Krogsgaard, M.; Behrens, M.A.; Pedersen, J.S.; Birkedal, H. Self-healing mussel-inspired multi-pH-responsive hydrogels. *Biomacromolecules* **2013**, *14*, 297–301. [CrossRef] [PubMed]
12. Cordier, P.; Tournilhac, F.; Soulié-Ziakovic, C.; Leibler, L. Self-healing and thermoreversible rubber from supramolecular assembly. *Nature* **2008**, *451*, 977. [CrossRef] [PubMed]
13. Burattini, S.; Greenland, B.W.; Merino, D.H.; Weng, W.; Seppala, J.; Colquhoun, H.M.; Hayes, W.; Mackay, M.E.; Hamley, I.W.; Rowan, S.J. A healable supramolecular polymer blend based on aromatic π−π stacking and hydrogen-bonding interactions. *J. Am. Chem. Soc.* **2010**, *132*, 12051–12058. [CrossRef] [PubMed]
14. Bode, S.; Zedler, L.; Schacher, F.H.; Dietzek, B.; Schmitt, M.; Popp, J.; Hager, M.D.; Schubert, U.S. Self-healing polymer coatings based on crosslinked metallosupramolecular copolymers. *Adv. Mater.* **2013**, *25*, 1634–1638. [CrossRef] [PubMed]
15. Nakahata, M.; Takashima, Y.; Yamaguchi, H.; Harada, A. Redox-responsive self-healing materials formed from host–guest polymers. *Nat. Commun.* **2011**, *2*, 511. [CrossRef] [PubMed]
16. Zhang, M.; Xu, D.; Yan, X.; Chen, J.; Dong, S.; Zheng, B.; Huang, F. Self-healing supramolecular gels formed by crown ether based host–guest interactions. *Angew. Chem. Int. Ed.* **2012**, *51*, 7011–7015. [CrossRef] [PubMed]
17. Wang, Q.; Mynar, J.L.; Yoshida, M.; Lee, E.; Lee, M.; Okuro, K.; Kinbara, K.; Aida, T. High-water-content mouldable hydrogels by mixing clay and a dendritic molecular binder. *Nature* **2010**, *463*, 339. [CrossRef] [PubMed]
18. Zhang, D.L.; Ju, X.; Li, L.H.; Kang, Y.; Gong, X.L.; Li, B.J.; Zhang, S. An efficient multiple healing conductive composite via host–guest inclusion. *Chem. Commun.* **2015**, *51*, 6377–6380. [CrossRef] [PubMed]
19. Wang, C.; Meng, D.; Sun, J.; Memon, J.; Huang, Y.; Geng, J. Graphene wrapped TiO_2 BASED CATALYSTS with enhanced photocatalytic activity. *Adv. Mater. Interfaces* **2014**, *1*, 1300150. [CrossRef]
20. Wu, Y.; Zuo, F.; Zheng, Z.; Ding, X.; Peng, Y. A novel approach to molecular recognition surface of magnetic nanoparticles based on host–guest effect. *Nanoscale Res. Lett.* **2009**, *4*, 738. [CrossRef] [PubMed]